

Application of gamma ray spectrometry in discovering the granitic monument of King Pepi I: a case study from Hierakonpolis, Aswan, Egypt

Akram Aziz^{*1}, Tamer Attia¹, Liam McNamara², Renee Friedman²

Dr. Akram Aziz ^{*1}

Assistant professor, Geology Department
Faculty of Science, Port Said University, Port Said, Egypt

Dr. Tamer Attia ¹

Assistant professor, Geology Department
Faculty of Science, Port Said University, Port Said, Egypt

Dr. Liam McNamara ²

Lisa and Bernard Selz Curator for Ancient Egypt and Sudan
Ashmolean Museum, University of Oxford

Dr. Renee Friedman²

Director, Hierakonpolis Expedition
Ashmolean Museum, University of Oxford

¹ Faculty of Science, Port Said University, Port Said, Egypt

² Ashmolean Museum, University of Oxford, UK

*Correspondence address: to Dr. Akram Mekhael Aziz via ghataas@gmail.com

Abstract

The current survey aimed to relocate the so-called granitic ‘stela’ inscribed for King Pepi I. The monument was originally discovered in 1897-98 by British Egyptologists excavating on an ancient mound located in the floodplain at the archaeological site of Hierakonpolis (modern Kom el-Ahmar), in the Aswan Governorate of Egypt. The original excavators were unable to remove it owing to its great weight and the monument was therefore left at the site. It remained partly exposed until 1989, when it was reburied in order to provide some protection from seasonal fluctuations in the water table. The exact location of the ‘stela’ was then lost, as the site is situated in the center of the modern village of Kom el-Gemuwia and is covered with halfa grass and other debris. As part of a new project to conserve and record this historic monument and other stone relics on this water-logged site by the Hierakonpolis Expedition of the Ashmolean Museum, University of Oxford, UK, a geophysical approach was used to establish their current locations. A detailed Gamma Ray Spectrometry survey was conducted across the area suggested by the archeologists. The measurements were analyzed and plotted in the form of maps, which were helpful in selecting certain locations for examination. The results of limited field excavations confirmed that the localized high Thorium concentration anomalies were mainly related to the presence of the buried granite block. These results suggest that this method could be useful in for the detection of granitic monuments at similar sites.

Keywords: Gamma Ray Spectrometry – Radioactive Dose Rate – Principle Component Analysis – Granitic monuments – King Pepi I.

Introduction

Gamma ray spectrometry (GRS) is a geophysical method used for detecting Natural Occurring Radioactive (NOR) mineralization and locating economically important minerals such as gold, tin and tungsten, which are often associated with the NOR elements (Shives et al. 2000; Wemegah et al. 2015). It is also utilized as a complementary method in regional geological mapping and fault delineation (Menager et al. 1993). Recently it has proven its efficiency in mapping areas of potential natural radiation hazards due to long term exposure to high radiation dose rates or terrestrial radon emission (Kaiser et al. 2014). GRS surveys are also carried out periodically around nuclear reactors or open-pit mines to monitor any accidental leakages of radioactive material into the surrounding environment (Erdi-Krausz et al. 2003). The current study aims to introduce the GRS method as a new tool in archaeological prospection. Using this method, the study succeeded in locating the granitic monument of King Pepi I (c. 2289–2255 BC) in an efficient manner.

Area of study

The site known to the ancient Greeks as Hierakonpolis, the ‘City of the Hawk’, is situated on the west bank of the Nile, c. 650 km south of Cairo and 17 km north-west of Edfu in Upper Egypt (Figures 1a and 1b). Its ancient Egyptian name was *Nekhen* and it is generally known today as Kom el-Ahmar. A major population and political center during the Predynastic and Early Dynastic periods (c. 3800–2800 BC), the site continued to be inhabited into the Roman period (Friedman 2011, 2013). The current survey was carried out at a low mound located in the floodplain constituting the remains of the Dynastic town (Figure 1c), which was first excavated by the British Egyptologists James Quibell and Frederick Green in 1897–1899 (Quibell and Green 1902; Adams 1995). Their work in the floodplain site revealed a rich temple precinct including many phases of stone and mud-brick architecture as well as important ancient artifacts, such as the famous Palette of Narmer (McNamara 2008).

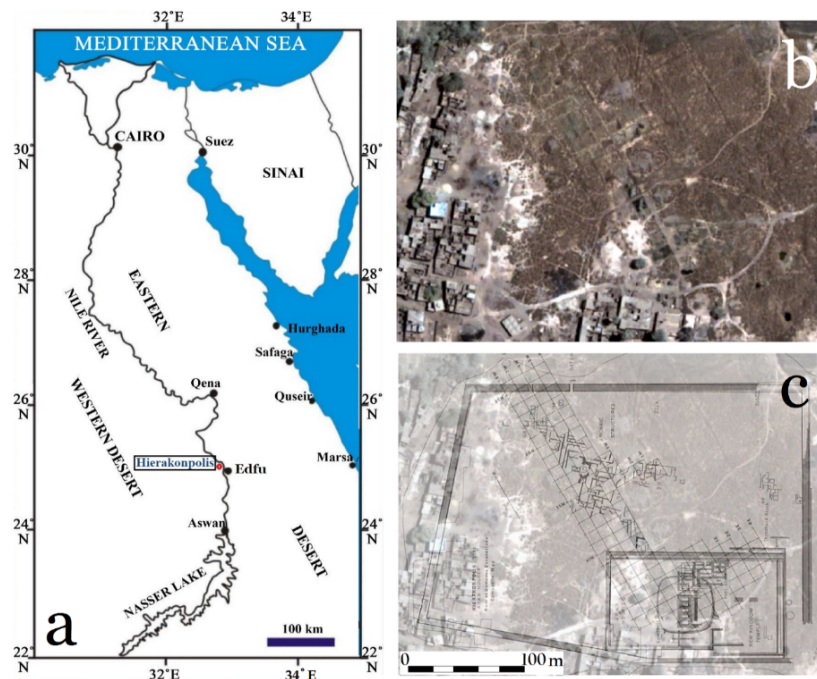


Figure 1: a) Map showing the location of Hierakonpolis; b) Satellite image of the floodplain mound at Hierakonpolis; c) Map showing the results of archaeological excavations 1897–1986 on the mound, modified after (Quibell and Green 1902; Fairservis 1986), overlaid on the satellite image.

The archaeological remains at Hierakonpolis are now under threat due to the expansion of irrigated agricultural land surrounding the site. As a result, the regional water table has risen significantly and the surface is waterlogged in some locations (Stearns 2006; El-Shishtawy et al. 2013). As part of a project to conserve the ancient stone monuments on the temple-mound, the archaeological mission of the

Ashmolean Museum, University of Oxford, UK, wished to relocate the granite monument of King Pepi in order to assess its condition. This 'stela' had been discovered in 1897 and photographed (Figure 2a), but despite its importance, it was never fully recorded. Seasonal fluctuations in the water table and highly salinated water are particularly damaging to granitic rock, while also enabling the rapid growth of halfa grass (see Figure 2c) which causes further damage to the archaeological remains. In 1989 the block was observed partly exposed in salt encrusted waterlogged soil (Figure 2b). It was then buried in an attempt to minimize further salt efflorescence. Owing to the heavy overgrowth of vegetation and other modifications to the site, the exact location of the monument was subsequently lost.

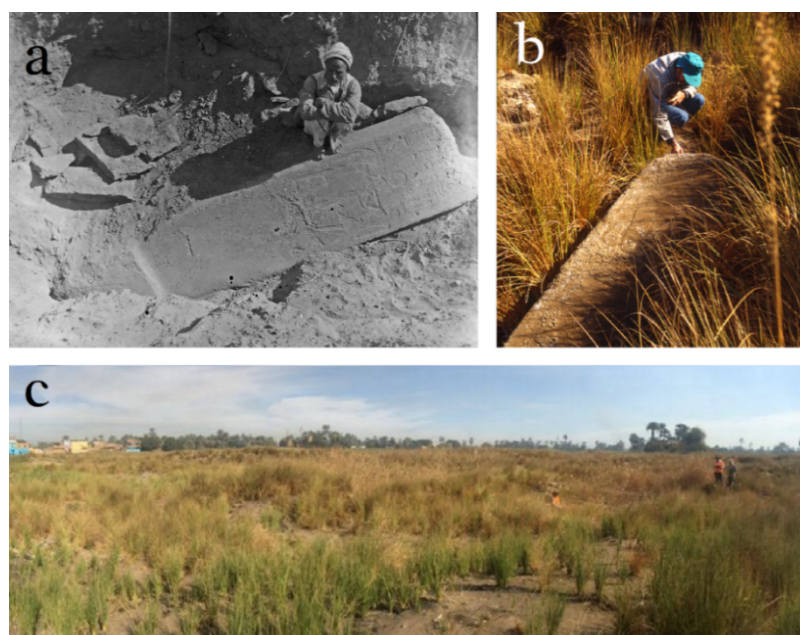


Figure 2: a) Archival photograph of the 'stela' of King Pepi as discovered in 1897 (courtesy of the Petrie Museum of Egyptian Archaeology, University College London; b) The 'stela' in 1989 before reburial (courtesy of the Hierakonpolis Expedition); c) The condition of the temple-mound in 2018.

Methodology and instrumentation

Igneous granitic rocks are generally enriched in Uranium (U^{238}) and Thorium (Th^{232}), especially if compared with other igneous basaltic or ultramafic rocks. In granites, the average abundance of Uranium is 5 ppm, and that of Thorium is 25 ppm. In ultramafic rocks, Uranium concentrations do not exceed 1 ppm and the average concentration of Thorium hardly reaches 3 ppm (Mussett and Khan 2000; Tzortzis et al. 2003). On the other hand, the abundances of these radioactive elements in sedimentary rocks and soils vary according to the source from which they derive. For instance, shale is considered as the highest radioactive sedimentary rock, where the Uranium average is 4 ppm and the Thorium average is 12 ppm (Dickson and Scott 1997; Mussett and Khan 2000). Moreover, shale and clay are naturally

containing minerals that have high potassium content, which consequently increases the total radioactivity of the clay and shale layers (Dickson and Scott 1997; Reynolds 2011).

The three preceding elements, K^{40} , U^{238} , and Th^{232} , are commonly known as Naturally Occurring Radioactive (NOR) elements. They are able to emit gamma radiation during their disintegration. This can be detected using modern gamma ray spectrometers such as the RS-230 Super-Spec, which was used in the current study. This instrument is able to record the gross radiation emissions from the NOR elements in a wideband energy channel, called the Total Count (TC) channel. It also has three separate sub-channels, each channel defined by upper and lower energy limits, in order to prevent the recording of gamma radiation emitted from sources other than the element specified (Erdi-Krausz et al. 2003).

Data acquisition

Based on the information provided by archaeologists about the dimensions of the buried 'stela' (its width being approximately one meter and its length more than four meters) a detailed surveying procedure was created to conduct the GRS ground survey. In total, 41 traverses, running parallel to each other and separated by 0.5m, were surveyed as shown in Figure (3a). The length of each traverse was 10 meters, and the distance between any two successive measuring stations along each line was 0.5 meter. The surveyed area covers 200 m² with 861 measured stations. The area of the survey is indicated by the yellow rectangle illustrated in Figure (3b). The elapsed time to measure each station was three minutes in order to allow the instrument to count the radiations in its internal sub-channels and then provide directly the Percentage of radioactive Potassium K^{40} in (%), the equivalent Uranium and Thorium in (ppm), and the Radioactive Dose Rate in ($\mu R/hr$), at each measured station. Results were then plotted in the form of maps, using Geosoft's Oasis-Montaj software version 8.4, showing the spatial distribution of each NOR element and their Total Dose Rate (Figure 4). The white ovals, shown in Figure (4), define the location of the lowest ground surface, in which the surveyor is standing in (Figure 3a). This area was also illustrated in Figure (5).

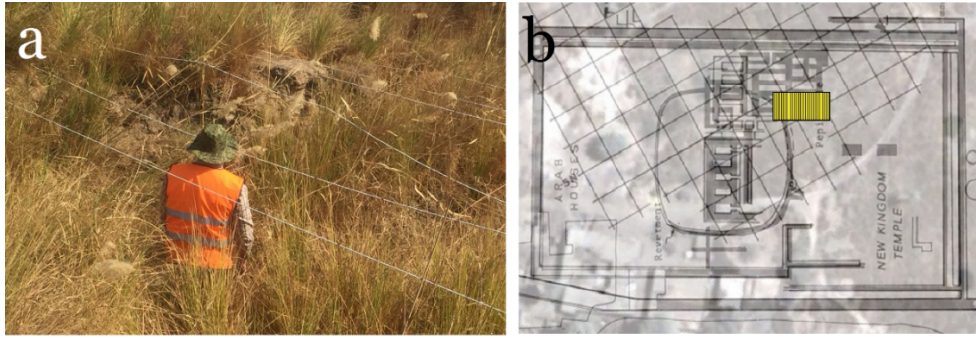


Figure 3: a) Laying out the grid in the field; station separation was 0.5m and traverses were spaced at 0.5m intervals; b) Plan of the surveyed grid within the Temple area; the yellow rectangle is the area surveyed using the gamma ray spectrometer.

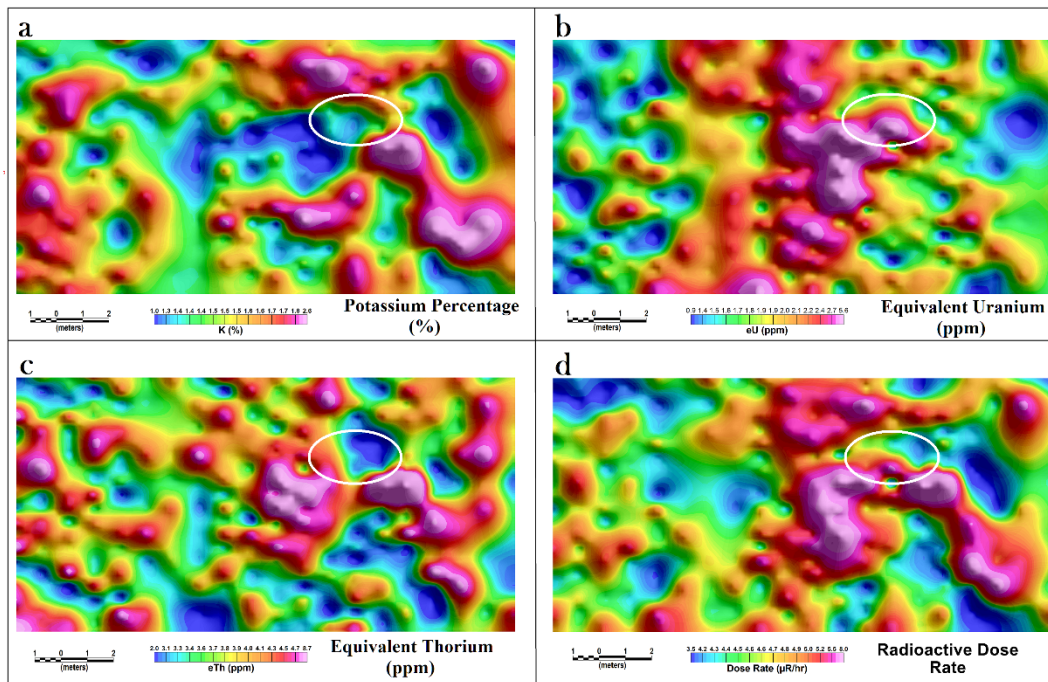


Figure 4: Spatial distribution maps of: a) Percentage of radioactive Potassium K^{40} in (%); b) Equivalent Uranium in (ppm); c) Equivalent Thorium in (ppm); d) Radioactive Dose Rate in ($\mu R/hr$). The white oval denotes the lowest ground surface in the survey area.

Results and discussion

Preliminary inspection of the maps (illustrated in Figure 4) revealed some interesting points. First, the Potassium percentage map (Figure 4a) shows a very significant low anomaly closure in the center of the area, while at the same corresponding location on the Uranium and Thorium maps (Figures 4c and 4d) high anomalies were detected. Conversely, high anomaly closures of Potassium, shown on the left side of the area, are occupied by low anomaly closures of Uranium. Field notes were very helpful in explaining this inverse relationship between Uranium and Potassium readings, especially on the left side of the area. During the field measurements, it was clearly noticed that the readings of the Potassium

percentages increased with the gradual rise in height of the ground surface towards the left side of grid. This gradual increment is due to accumulations of clay deposits. Therefore, the recorded measurements on the elevated left side of the grid show an increasing potassium percentages, due to the natural high potassium content in clay (Moussa 2001), at the expense of the other NOR elements.

The second observation to be discussed is the large longitudinal high anomaly that can be traced in the middle third of Uranium map in Figure (4b). Field observations showed that the ground surface at this part of the area is lower than the other areas within the survey grid. Salt crystals were seen on the ground surface, demonstrating that the center of this depression has been waterlogged owing to the seasonal fluctuations of the water table when the fields are flooded for cultivation (Figure 5).



Figure (5): Salt efflorescence in seasonally waterlogged depression at the center of the surveyed area.

Oxygen and acidic water are the main factors controlling the migration of Uranium from the outcrops of granitic rocks (Klepper and Wyant 1957). The frequent fluctuations in the water table across the surveyed area provides favorable conditions for Uranium to be leached from the granitic stone, which then sinks deep into the soil or subsoil and may follow subterranean drainage channels, whether in solution or adsorbed on particles of clay minerals (McKelvey and Nelson 1950). Uranium can then be re-deposited in new and perhaps much richer concentrations (Reynolds 2011). The highest concentration of Uranium is located at the middle-right side of the previously described longitudinal anomaly, shown in Figure (4b). This highest closure seems to be spatially close to the main radioactive source from which Uranium was leached. The intensity of the anomaly lowered and faded towards the right side of the grid, which implies that the Uranium has migrated in a subsurface drainage channel, or due to the increase of the alluvial deposits above it.

Also to be noted is the Thorium concentration map (Figure 4c), which shows two clear anomaly closures. The first is located in the middle part of the map and is almost circular in shape. Its location, as

stated previously, is occupied by the negative anomaly of Potassium, while it is overlaid by a high anomaly closure on the Uranium map. To the right of the first anomaly, another elongated anomaly can be seen, which is also clearly visible on the Potassium map, but hardly present on the Uranium map.

To facilitate the visual inspection of the relationship between multivariable data, which are commonly encountered in gamma ray spectrometry surveys, various methods could be utilized to combine the results in an uni-dimensional view. Estimating the gamma radiation Dose Rate (DR) is one of the most conventional procedures used for interpreting and enhancing the radiometric data by combining the effects of the three NOR elements in one display. The Dose Rate reflects the gross dose of gamma emissions per one hour, and can be calculated according to the following equation (Erdi-Krausz et al. 2003):

$$DR_{(\mu R/h)} = 1.505 (C_k) + 0.6535 (C_U) + 0.287 (C_{Th})$$

where, (C_k) is the percentage of K, (C_U) is the eU concentration in (ppm), and (C_{Th}) is the eTh concentration of in (ppm). The results are expressed in terms of micro Roentgen per hour ($\mu R/h$).

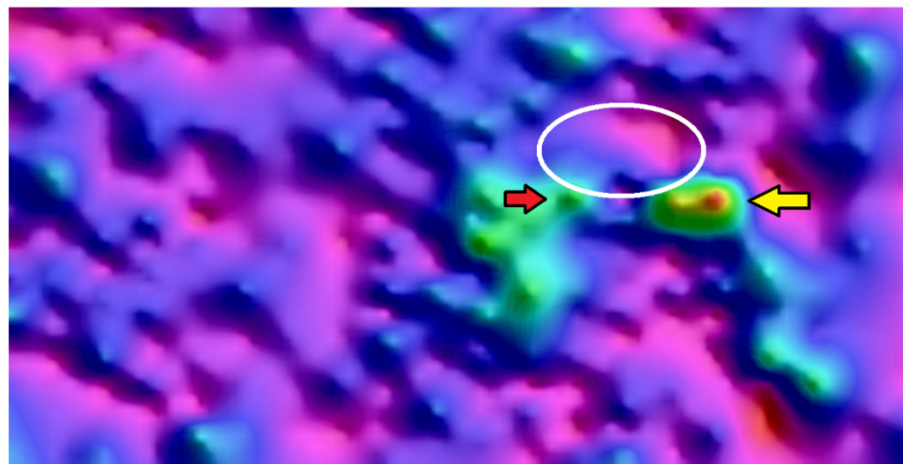
The method has been extensively employed in environmental studies, where it has been used to delineate areas of natural radiation hazards (Kaiser et al. 2014). Modern GRS instruments, such as the one used in the current study, implement this function to be calculated and displayed directly during the field measurements. The measured Dose Rates are illustrated in Figure (4d). As noted from the map, only the overlapping portions of the previously described NOR high anomalies have been enhanced. The resulting map was confusing, but it served to limit the area of interest to the eastern half of the grid. Another effective processing technique used for combining not only the NOR results but also their ratio and even the calculated Dose Rate, is Principal Component Analysis (PCA) (Manly and Alberto 2016). PCA highlights areas of high levels of correlation between DR, K, eU, and eTh. It is also able to reduce the noise or suppress the influence of less important data components, where weak or no correlations between variables exist (Raychaudhuri et al. 1999). It is not only able to delineate the surface distribution of the main source of radiation, but it is also able to define its underlying structure (Attia and Shendi 2013). The First Principal Component (PC1) was computed using the following equation with five positive weights of the variables K, DR, eTh, eTh/K and eU and two negative weights eU/K and eU/eTh:

$$PC1 = 0.21(K) + 0.26(DR) + 0.26(eTh) + 0.1(eTh/K) + 0.23(eU) - 0.08(eU/eTh) - 0.13(eU/K)$$

The computed results were mapped and are illustrated in Figure (6). The map clearly defined the boundaries between the highest and the lowest values of radioactivity. Two clear anomalies can be seen on the PC1 map. One of them shows a sharply rectangular-shaped positive anomaly with dimensions

very close to those of the upper portion of the buried granite block (2 m long and 1 m wide), denoted by a yellow arrow in Figure (6). The second anomaly is larger in size, but has no clear orientation like the first one. It is characterized by the presence of small circular-shaped positive anomalies at its edges. The red arrow shown in the figure points to the highest circular anomaly, located only 2 meters to the left of the rectangular anomaly.

Two orthogonal profiles, AB and CD were plotted and are illustrated in Figure (7) to show the lateral changes of eU, eTh and DR across the rectangular anomaly. The first profile AB runs perpendicular to the strike of the anomaly, and shows a symmetrical anomaly curve around its center. It was easy to locate the center of the buried body, directly under the highest value of the curve, while the width of the source body is equal to the distance between the two inflections on the two sides of each anomaly curve. The width of the body, as shown on the AB profile, is 1 m. The second profile, CD, runs along the anomaly. The curves here show a wider anomaly, as the distance between the two maximum inflections equals 1.9 m. The asymmetrical shape of the curve could be the result of two adjacent radioactive sources, or due to the presence of one elongated but inclined source.



1 0 1 2
(meters)

First Principal Component (PC1)

Figure 6: Mapped results of the computed First Principle Component (PC1).

Arrows are pointing to the recommended locations for ground truthing.

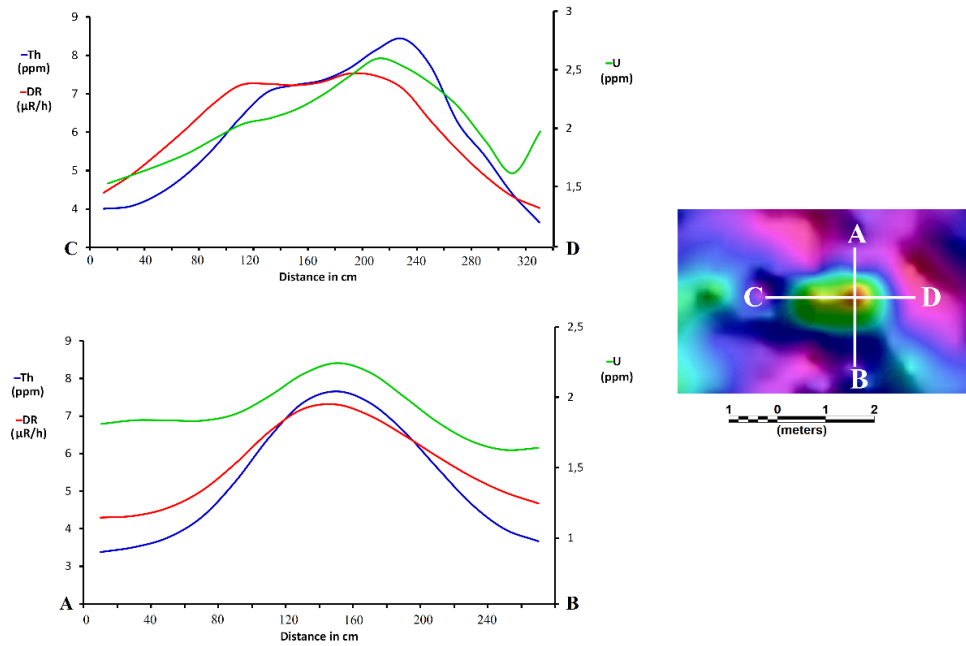


Figure 7: Two data curves illustrating the lateral variation in equivalent Uranium eU, equivalent Thorium eTh, and Dose Rate DR, across the rectangular anomaly.

Having defined the probable locations of the two anomalies, the overgrowth of halfa grass was removed and the site was examined under the supervision of the archaeologists, as shown in Figure (8a and b). The results show strong concordance with the interpreted results of the GRS data. Figure (8c) shows the monument after excavation, as well as the level of the local water table. It also shows how the lower end of the block is immersed in water. The damage caused by fluctuations in the water table is obvious and should be noted (see also (El-Shishtawy et al. 2013)). Once cleared and cleaned by conservation specialists from the Ashmolean Museum, University of Oxford, UK, all sides of the monument were studied, especially the upper surface, which is carved in sunk relief with scenes depicting the king standing in front of two deities. Another buried block was also observed at the location of the second anomaly, denoted by red arrow in the PC1 map (Figure 6), two meters to the left of the uncovered stela (Figure 8b). This previously unreported block is another piece from the monumental doorway, but it could not be investigated further at the current time. These discoveries are now important for understanding the architectural history of this ancient temple site. It also suggests that the monument was not a free standing stela as previously assumed, but instead was an inscribed door jamb since one side of the block was intentionally left unsmoothed. This side was presumably once built into a mud brick wall.



Figure 8: a) Defining the location of the target and removing the overgrowth of halfa grass; b) Archaeological clearance of the area to test the readings; c) The uncovered granite block with its lower end submerged at the level of the water table. Black arrows point to the lowest ground surface within the surveyed grid. Yellow arrows point to the exact location of the stela, and red arrow points to the location of another buried block.

Conclusion

A Gamma ray spectrometry survey was conducted with an intensive detailed survey design, on the town and temple mound at the archaeological site of Hierakonpolis (Kom el-Ahmar), Edfu, Aswan, in order to detect the buried granitic monument of King Pepi I. Equivalent Uranium and Thorium were measured and plotted on maps. The Uranium map showed more dispersed anomalies due to its mobility, which is greatly affected by the frequent fluctuations in the water table at the site. Thorium showed fewer localized anomalies than Uranium. On the other hand, Potassium was related more to the thickness of the alluvial deposits rather than being correlated with the radioactive source. Combining the results in

Dose Rate maps was not as helpful as the First Principle Component (PC1), which was very effective in defining the edges of the stone and determine its width, length and also its gradient. Analyzing the measured data along two profiles, crossing the main PC1 anomaly, enabled the team to determine the probable location of the buried monument. Clearance took place under the supervision of the Oxford University Team, and the results showed strong agreement with the interpreted radiometry measurements. The survey successfully introduces gamma ray spectrometry as a direct tool in archaeological prospection, especially for the detection of buried granitic blocks.

Acknowledgements

We are grateful to the Minister of State for Antiquities, Dr Khaled el-Anany and the members of the Permanent Committee of the Supreme Council for Antiquities for permission to undertake work at Hierakonpolis. Thanks is also extends to the PSU center of Environmental Studies and Consultancies. We are very grateful to Mr. Mahmoud Ismail for his valuable help and effort during the field surveys. The assistance of the Edfu Inspectorate of Antiquities is also gratefully acknowledged.

References

- Adams, B. (1995). Ancient Nekhen: Garstang in the city of Hierakonpolis: SIA. Whitstable.
- Attia, T. E., & Shendi, E. H. (2013). Uranium migration history in the igneous and metamorphic rocks of Solaf-Umm Takha area, based on multi-variate statistical analysis and favorability indices, central south Sinai, Egypt. IOSR J Appl Geol Geophys (IOSR-JAGG). e-ISSN, 2321-0990.
- Dickson, B., & Scott, K. (1997). Interpretation of aerial gamma-ray surveys-adding the geochemical factors. AGSO Journal of Australian Geology and Geophysics, 17, 187-200.
- El-Shishtawy, A., Atwia, M., El-Gohary, A., & Parizek, R. (2013). Impact of soil and groundwater corrosion on the Hierakonpolis Temple Town archaeological site, Wadi Abu Sufian, Idfu, Egypt. Environmental monitoring and assessment, 185(6), 4491-4511.
- Erdi-Krausz, G., Matolin, M., Minty, B., Nicolet, J., Reford, W., & Schetselaar, E. (2003). Guidelines for radioelement mapping using gamma ray spectrometry data: also as open access e-book: International Atomic Energy Agency (IAEA).
- Fairservis, W. (1986). The Hierakonpolis Project. Season January to May 1981. Occasional Papers in Anthropology III, Vassar College, Poughkeepsie, NY.
- Friedman, R. (2011). Hierakonpolis. In Teeter, E. (ed.), Before the Pyramids. The origins of Egyptian civilization. Oriental Institute Pub. 33. Chicago: 33-44. <http://oi.uchicago.edu/pdf/oimp33.pdf>.
- Friedman, R. (2013). Hierakonpolis. The Encyclopedia of Ancient History, Wiley Online.
- Kaiser, M., Aziz, A., & Ghieth, B. (2014). Environmental hazards and distribution of radioactive black sand along the Rosetta coastal zone in Egypt using airborne spectrometric and remote sensing data. Journal of environmental radioactivity, 137, 71-78.
- Klepper, M. R., & Wyant, D. G. (1957). Notes on the geology of uranium: US Government Printing Office.
- Manly, B. F., & Alberto, J. A. N. (2016). Multivariate statistical methods: a primer: Chapman and Hall/CRC.
- McKelvey, V. E., & Nelson, J. M. (1950). Characteristics of marine uranium-bearing sedimentary rocks. Economic Geology, 45(1), 35-53.
- McNamara, L. (2008). The revetted mound at Hierakonpolis and early kingship: a re-interpretation. In Midant-Reynes, B & Tristant, Y. (eds), Egypt at its origins 2. Proceedings of the International Conference "Origin of the state, Predynastic and Early Dynastic Egypt", Toulouse (France), 5th-8th September 2005: Leuven: 901-936. Menager, M., Heath, M., Ivanovich, M., Montjotin, C., Barillon, C., Camp, J., et al. (1993). Migration of uranium from uranium-mineralised fractures into the rock matrix in granite: implications for radionuclide transport around a radioactive waste repository. Radiochim. Acta, 66(67), 47-83.

- Moussa, M. (2001). Gamma-ray spectrometry: a new tool for exploring archaeological sites; a case study from East Sinai, Egypt. *Journal of Applied Geophysics*, 48(3), 137-142.
- Mussett, A. E., & Khan, M. A. (2000). *Looking into the earth: an introduction to geological geophysics*: Cambridge University Press.
- Quibell, J. E., & Green, F. W. (1902). *Hierakonpolis: Part II: Quaritch*. London.
- Raychaudhuri, S., Stuart, J. M., & Altman, R. B. (1999). Principal components analysis to summarize microarray experiments: application to sporulation time series. In *Biocomputing 2000* (pp. 455-466): World Scientific.
- Reynolds, J. M. (2011). *An introduction to applied and environmental geophysics*: John Wiley & Sons.
- Shives, R. B., Charbonneau, B., & Ford, K. L. (2000). The detection of potassic alteration by gamma-ray spectrometry—Recognition of alteration related to mineralization detecting Ore Using GRS and K Alteration. *Geophysics*, 65(6), 2001-2011.
- Stearns, A. D. (2006). *Effects of Large Irrigation Projects on Regional Ground Water Chemistry Near Hierakonpolis, Egypt*. PhD diss., Pennsylvania State University.
- Tzortzis, M., Tsertos, H., Christofides, S., & Christodoulides, G. (2003). Gamma radiation measurements and dose rates in commercially-used natural tiling rocks (granites). *Journal of environmental radioactivity*, 70(3), 223-235.
- Wemegah, D. D., Preko, K., Noye, R. M., Boadi, B., Menyeh, A., Danuor, S. K., et al. (2015). Geophysical interpretation of possible gold mineralization zones in Kyerano, south-western Ghana using aeromagnetic and radiometric datasets. *Journal of Geoscience and Environment Protection*, 3(04), 67.